Iranian Polymer Journal
**18** (5), 2009, 401-413

Available online at: http://journal.ippi.ac.ir

# Preparation of High-performance Damping Materials Based on Carboxylated Nitrile Rubber: Effects of Organic Fillers

Qixia Liu, Huiping Zhang, and Xiong Yan*

Key Laboratory of Textile Science and Technology, Ministry of Education,
College of Textiles, Donghua University, Shanghai, 201620, PR China

Received 15 December 2008; accepted 4 April 2009

## A B S T R A C T

Several novel organic hybrid systems based on carboxylated nitrile rubber (XNBR) were prepared. The damping properties of organic hybrids consisting of XNBR, 2,2'-methylenebis(6-*t*-butyl-4-methylphenol) (AO-2246), and pentaerythrityl-tetrakis-[β(3,5-di-*t*-butyl-4-hydroxyphenyl)-propionate] (AO-1010) were investigated by dynamic mechanical analysis (DMA). Binary XNBR/AO-2246 system was compatible and showed only one damping peak associated with XNBR, whereas binary XNBR/AO-1010 system was partially compatible and a new damping peak appeared besides that of XNBR. FTIR measurements and SEM observation were carried out to clarify the molecular mechanism of the different additive effects of AO-2246 and AO-1010. DMA results of ternary XNBR/AO-2246/AO-1010 systems showed that the addition of a small amount of AO-1010 into XNBR/AO-2246 further enhanced the damping peak height and peak temperature remarkably, demonstrating that combined AO-2246 and AO-1010 had a synergistic effect on improving the damping property of XNBR. Furthermore, studies on the damping stability of such organic hybrids during ageing and annealing process revealed that the addition of small amount of AO-1010 into XNBR/AO-2246 obstructed the crystallization behaviour of AO-2246 and finally improved the damping stability. Thus, a series of XNBR-based high-performance damping materials with high damping peak and controllable peak position as well as better damping stability were obtained.

**Key Words:**

carboxylated nitrile rubber (XNBR);
hindered phenol;
organic hybrids;
hydrogen bond;
damping property.

(*) To whom correspondence to be addressed.
E-mail: yaxi@dhu.edu.cn

## INTRODUCTION

Polymers are seldom used commercially in a pure state, because it is often necessary for some of their properties to be modified by adding various additives, such as fillers, vulcanizing agents, and plasticizers etc. [1-9]. Mixtures of a polymer with such additives were previously investigated extensively in very low concentration range, where the polymer was the major component. However, much less studies have been devoted to the moderate concentration range, where the content of the additives is close to or greater than that of the polymer. Recently, Wu et al. have reported that addition of a large amount of some functional small molecular organic compounds such as vulcanization accelerator, hindered amine, and hindered phenol compounds into polar polymers would give rise to some unknown useful functions, such as super damping, shape-memorization, self-adhesiveness and self-restoration, especially the super damping properties

[10-18]. These new types of organic hybrid damping materials designed are based on the sophisticated use of hydrogen bonds and have attracted much research attention [19-21].

For such organic hybrid damping systems, the selection of matrix polymers and low molecular organic substances is of vital importance. Compatibility between the two components plays an important role in determining the damping properties of the system. Polar polymers such as chlorinated polyethylene (CPE), chlorinated polypropylene (CPP), and acrylate rubber (ACM) have been reported as common matrix polymers while chlorinated butyl rubber (CIIR) [22] and epoxidized natural rubber (ENR) [23] as well as nitrile butadiene rubber (NBR) [24] have recently been reported as matrix polymers in organic hybrid systems for the first time. Carboxylated nitrile rubber (XNBR) is a modified NBR with carboxylic groups along the hydrocarbonate chain [25]. Compared with NBR, XNBR is more polar, and it shows good compatibility with polar or non-polar resins and higher degree of interaction with fillers [26]. It is also reported that XNBR has improved damping properties, showing a great potential as matrix polymers [27,28].

However, until now no reports have been made on the use of XNBR employed as matrix polymer in organic hybrid systems. With this work, we intend to partially fill this gap. Therefore, in this study, based on the new design concept of organic hybrid damping materials, XNBR was chosen for the first time as the polar matrix polymer to develop a new XNBR-based organic hybrid system with high-performance damping properties and also to extend the application field of XNBR into organic hybrid systems. The new XNBR-based organic hybrids are prepared by adding a large amount of polar organic hindered phenol compounds 2,2'-methylenebis(6-*t*-butyl-4-methylphenol) (AO-2246) and pentaerythrityl-tetrakis-[β-(3,5-di-*t*-butyl-4-hydroxyphenyl)-propionate] (AO-1010) into XNBR matrix. Our design concept is to obtain a uniformly dispersed polymer/small molecular system by adjusting the processing parameters during the blending process of a large amount of AO-2246 or AO-1010 with XNBR. Thus the two components would be hybridized due to the formation of interactive reversible hydrogen bonding between them. The dissociation and rebuilding of intermolecular hydrogen bonding dissipate a great amount of mechanical energy as heat formation, thus will bring high damping properties. The additive effects of AO-2246 or/and AO-1010 on the damping properties of XNBR were first investigated and the molecular mechanism of different systems were discussed and indications were made to further studies on organic hybrid damping materials. The damping stability of these hybrid systems during ageing and annealing processes was subsequently investigated to obtain some ideas on their application potential in long-term practical service.

## EXPERIMENTAL

### Materials

The XNBR used as matrix in this study, with an acrylonitrile degree of 40 wt% and a carboxyl degree of 3 wt%, is a powdered rubber (manufactured by Nanjing Shengdong Chemical Co., Ltd., China). The organic low molecular weight hindered phenols AO-2246 and AO-1010, as shown in Scheme I, are commercially available antioxidants (supplied by Nanjing Hua Lim Co., Ltd., China).

### Samples Preparation

XNBR powders were first kneaded for 5 min at ca. 60°C on a laboratory size two-roll mixing mill. Then different weight fractions of AO-2246 or/and AO-1010 were incorporated into the kneaded XNBR and blended further for another 15-30 min depending on different loadings. No other rubber additives such as plasticizer, vulcanizing agent, cross-linking agent were used. The mixtures were preheated at 140°C for 5 min under a low pressure of 1 MPa and then compression moulded for 10 min under a high pressure of 10 MPa using a small laboratory press. Finally, the moulded samples were removed immediately and quenched by ice water to obtain sheets with a thickness of about 1 mm.

### Measurements

*Dynamic Mechanical Analysis (DMA)*

The dynamic mechanical measurements were carried out using a dynamic mechanical analyzer (DMA-7,

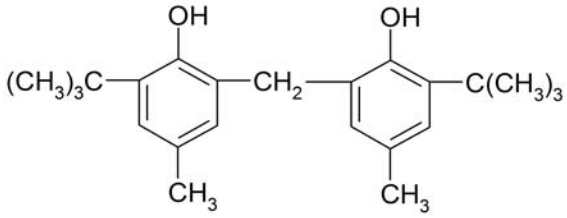

(a)

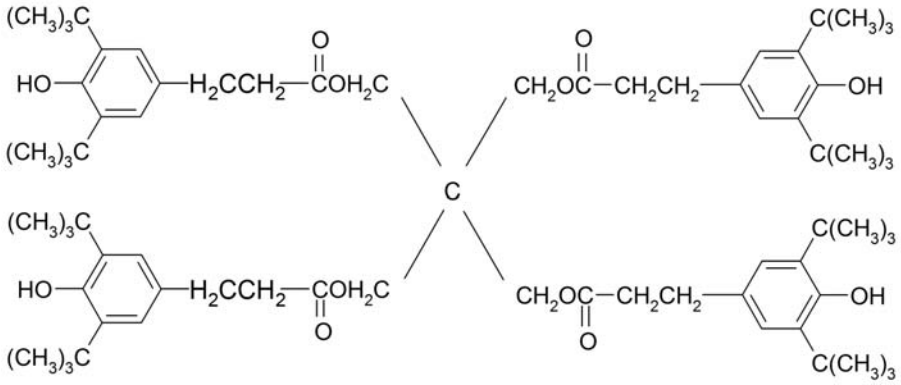

(b)

**Scheme I.** Chemical structures of: (a) AO-2246 and (b) AO-1010.

Perkin Elmer) in a tension mode on parallelepiped samples of the following dimensions: 12 mm long, 4 mm wide, and around 1 mm thickness. The temperature dependence of loss tangent (tan δ) for various samples was measured between -50°C and 100°C at a constant frequency of 1 Hz and a heating rate of 5°C/min.

*Scanning Electron Microscopy (SEM)*

SEM observation was performed with a Jeol JSM-5600LV apparatus to investigate the dispersion state of AO-2246 or AO-1010 in XNBR matrix. Prior to SEM observations, liquid nitrogen fractured surfaces of the composites were gold sputtered.

*Fourier Transform Infrared (FTIR) Spectroscopy*

Infrared measurements were conducted on a Nicolet 5700 FTIR spectrometer. The FTIR spectra were obtained by scanning the specimens in the wavenumber range from 400 $cm^{-1}$ to 4000 $cm^{-1}$ for 64 times with a resolution of 2 $cm^{-1}$. The FTIR spectra of as-received AO-2246 and AO-1010 powders were acquired by using ultra-thin disk specimens pressed from AO-2246 or AO-1010 ground in anhydrous potassium bromide (KBr). The FTIR spectra of XNBR/AO-2246 and XNBR/AO-1010 composites were acquired from sheet specimens with a thickness of approximately 1 mm, using the attenuated total reflection (ATR) technique.

*Optical Microscopic Observation*

The shapes of AO-2246 crystals formed at the surfaces of various samples during annealing process were observed under a HIROX 3-D rotational digital video microscopy (KH-1000, Questar) with a fixed magnification of 80.

## RESULTS AND DISCUSSION

### Additive Effects of Hindered Phenols on Damping Properties of XNBR

The damping properties of XNBR-based organic hybrids are investigated by means of DMA analysis and loss tangent (tan δ) is used as a measure of damping. Figure 1 shows the temperature dependence of tan δ for XNBR/AO-2246 samples with various weight ratios of AO-2246. As shown in this figure, all

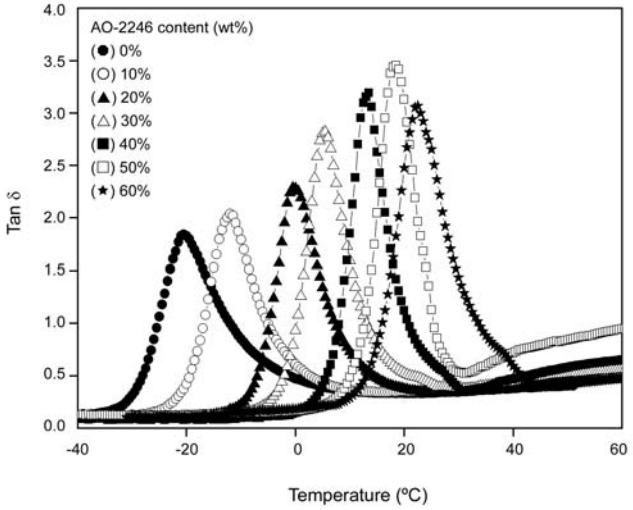


**Figure 1.** Temperature dependence of tan δ at 1 Hz for XNBR/AO-2246.

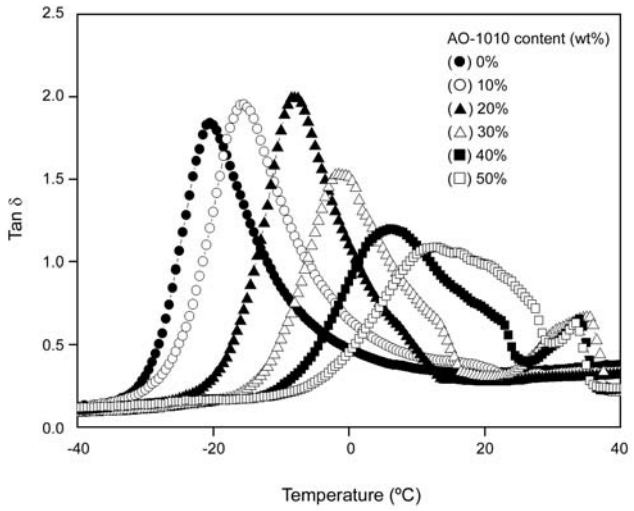


**Figure 2.** Temperature dependence of tan δ at 1 Hz for XNBR/AO-1010.

the XNBR/AO-2246 blends show a single tan δ peak associated with $T_g$ of XNBR. With increasing AO-2246 content, the tan δ peak height increases and its peak position shifts to higher temperatures. The growth and peak shift of the tan δ peak in the XNBR/AO-2246 blends demonstrate that AO-2246 is compatible with XNBR. Moreover, we note that when AO-2246 content in the blends increases from 0% to 60%, the tan δ peak maximum value increases remarkably from 1.8 up to 3.5 which then it decreases. The decrease of the tan δ peak height at a higher AO-2246 content is due to the crystallization of some excess AO-2246 molecules. Meanwhile, the damping peak temperature ($T_g$) increases significantly from -21°C to 23°C approaching room temperature, resulting in that XNBR/AO-2246 composite is a promising damping material.

By contrast, in the case of XNBR/AO-1010, as shown in Figure 2, with increasing AO-1010 content, the tan δ peak associated with $T_g$ of XNBR first increases slightly and then it decreases sharply and blends with a larger AO-1010 content than 20%, which clearly exhibits two tan δ peaks, indicating that AO-1010 is partially compatible with XNBR. We note that though the first tan δ peak height decreases sharply with increasing AO-1010 content, the tan δ value between the two tan δ peaks increases gradually, showing a broader efficient damping temperature region. Moreover, the tan δ peak position of the first tan δ peak shifts significantly towards room temperature while the position of the second tan δ peak is nearly unchanged.

As it is stated above, the design concept of such organic hybrids consisting of polar polymers and hindered phenol compounds is based on the use of interactive hydrogen bond between the two compounds. In order to clarify why there is such a big difference in the additive effects of AO-2246 and AO-1010 on the damping properties of XNBR, various types of hydrogen bonding interactions formed in the two systems were investigated by FTIR measurement. The infrared spectra centered near 3500 $cm^{-1}$ corresponding to hydroxyl group (OH) stretching region and that corresponding to nitrile group (C≡N) stretching region (2200-2300 $cm^{-1}$) as well as carbonyl group (C=O) stretching region (1650-1850 $cm^{-1}$) for various samples are shown in Figures 3 and 4, respectively. The peak intensity is normalized by the peak height of the C-H stretching vibration at 2954 $cm^{-1}$.

As shown in Figure 3, in the spectrum of pure AO-1010, there exist a narrow band at 3643 $cm^{-1}$ and a broad band at 3465 $cm^{-1}$, which can be assigned to free (non-hydrogen bonded) OH groups and OH–C=O (hydrogen bonded) interaction between AO-1010 molecules, respectively. For the XNBR/AO-1010 (40%) sample, the two bands decrease sharply and a new band at 3598 $cm^{-1}$ appears. As seen in Figure 4, in XNBR/AO-1010 (40%) system, the band

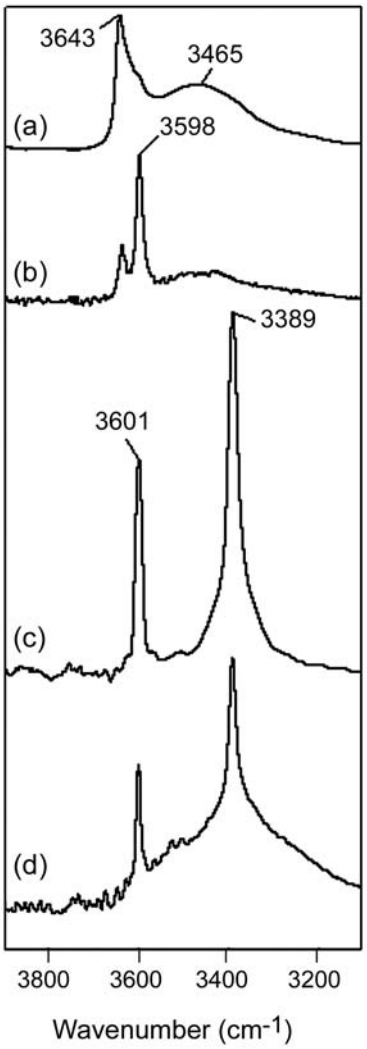


**Figure 3.** Infrared spectra in the OH stretching region for various samples: (a) pure AO-1010, (b) XNBR/AO-1010 (40%), (c) pure AO-2246, and (d) XNBR/AO-2246 (40%).

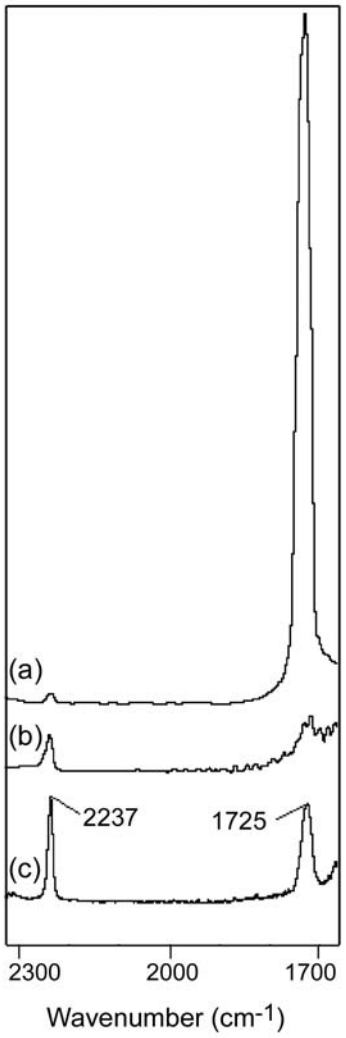


**Figure 4.** Infrared spectra in the CN as well as C=O stretching region for various samples: (a) XNBR/AO-1010 (40%), (b) XNBR/AO-2246 (40%), and (c) neat XNBR.

at 2237 $cm^{-1}$ corresponding to C≡N of XNBR becomes very small and the band at 1725 $cm^{-1}$ corresponding to C=O of XNBR becomes extremely large, which indicate that by addition of AO-1010 into XNBR, the number of free C≡N groups decreases sharply while the number of free C=O groups increases remarkably. The increase of free C=O groups is attributed to the dissociation of OH–C=O intermolecular hydrogen bonds between AO-1010 molecules which releases some C=O and OH groups. However, the band at 3643 $cm^{-1}$ corresponding to free OH groups decreases sharply rather than increases. Thus it can be deduced that the new band at 3598 $cm^{-1}$ may be assigned to OH–C≡N intermolecular hydrogen bond between C≡N of XNBR and free OH as well as released OH of AO-1010 molecules.

It can also be seen from Figure 3 that the salient feature of the spectrum of pure AO-2246 is the presence of two sharp absorption bands associated with the OH group stretching vibration. The band at 3601 $cm^{-1}$ is assigned to free OH groups, whereas the band at 3389 $cm^{-1}$ is assigned to the OH–OH intermolecular hydrogen bonds between AO-2246 molecules. For XNBR/AO-2246 (40%) sample, the two bands both decrease while a new broad band appears, indicating that some new types of hydrogen bond may be formed. As shown in Figure 4, compared with XNBR, the band at 2237 $cm^{-1}$ corresponding to C≡N and the

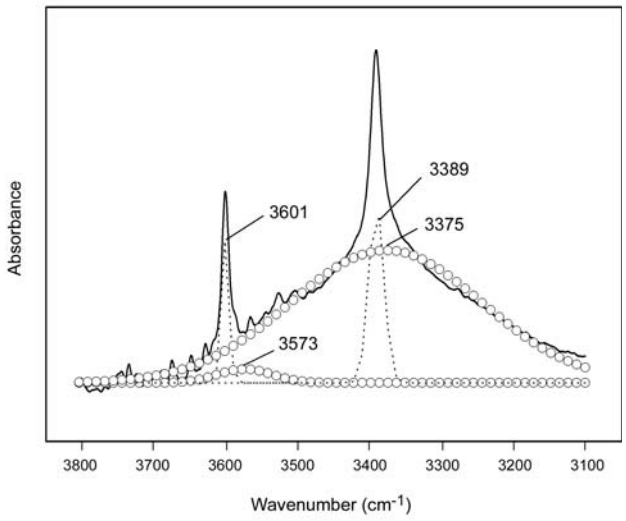


**Figure 5.** Gauss fit curves of infrared spectra in the OH stretching region for XNBR/AO-2246 (40%).

band at 1725 $cm^{-1}$ corresponding to C=O of XNBR/AO-2246 (40%) sample both become smaller. This indicates that by addition of AO-2246, the number of free C≡N and C=O groups of XNBR decreases, which may be caused by the formation of intermolecular hydrogen bond with OH groups of AO-2246.

To further elucidate the various intermolecular hydrogen bonding interactions in XNBR/AO-2246 (40%) system, a peak fit process, in which the Gaussian equation is used, was performed on its infrared spectra in the OH group stretching region (3100-3800 $cm^{-1}$). The gauss fit curves of the two peaks are shown in Figure 5. As it is observed in this figure, in addition to the two sharp bands at 3601 and 3389 $cm^{-1}$, as exist in pure AO-2246, two new broad bands appear at 3573 and 3375 $cm^{-1}$, respectively. According to what has been discussed above, the small broad band at 3573 $cm^{-1}$ can be assigned to the OH–C=O intermolecular hydrogen bond between C≡N of XNBR and OH of AO-2246 molecules and the much larger broad band centered at 3375 $cm^{-1}$ can be assigned to the OH–C=O intermolecular hydrogen bond between C=O of XNBR and OH of AO-2246 molecules.

From the above analysis, we can confirm that different types of intermolecular hydrogen bonds are formed between XNBR and AO-1010 or AO-2246 of the two systems. By further comparing the intensity and location of the absorption bands corresponding to these hydrogen bonds, we find that addition of AO-1010 brings about a new narrow band at 3598 $cm^{-1}$, while the addition of AO-2246 brings about a large broad band centered at 3375 $cm^{-1}$ besides a small broad band centered at 3573 $cm^{-1}$. This indicates that the few intermolecular hydrogen bonding interactions formed in XNBR/AO-1010 are weak, while those formed in XNBR/AO-2246 system are more and much stronger. The differences in the number and strength of the intermolecular hydrogen bonds in the two systems may lead to different dispersion states of AO-2246 and AO-1010 in XNBR matrix, which will finally result in different additive effects on damping properties of XNBR. To confirm this, SEM observation was performed on different samples.

The SEM photographs of XNBR/AO-2246 (40%) and XNBR/AO-1010 (40%) samples are compared with that of neat XNBR in Figure 6. As shown in the figure, the fracture surface of neat XNBR is quite smooth and some tiny particles, which can be attributed to the talc powders and calcium carbonate added as the dusting agents during the producing process of XNBR, are observed. However, in the XNBR/AO-2246 system, all the AO-2246 molecules and XNBR are hybridized due to the strong intermolecular hydrogen bonding interactions between them, as demonstrated by the special flower-like morphology. Thus, only one tan δ peak appears in the tan δ-T curve and both the peak height and the peak temperature are remarkably increased as a result of the hybridization effect. Whereas, in the XNBR/AO-1010 system, most of the AO-1010 molecules are dispersed in the XNBR matrix in the form of crystal particles or aggregates and the system exhibits a sea (XNBR-rich matrix)-island (AO-1010-rich domain) morphology due to weak interaction between AO-1010 and XNBR. As a result, a new tan δ peak appears besides that of XNBR. According to the above FTIR analysis, appearance of the new small tan δ peak seems to be due to the relatively weak OH–C≡N intermolecular hydrogen bonding interaction between XNBR and AO-1010 within the AO-1010-rich domain in which some XNBR chains are incorporated. Meanwhile, the AO-1010-rich domain, which is mainly composed of AO-1010 crystals, seems to act as inorganic fillers and decreases the tan δ peak of XNBR significantly.

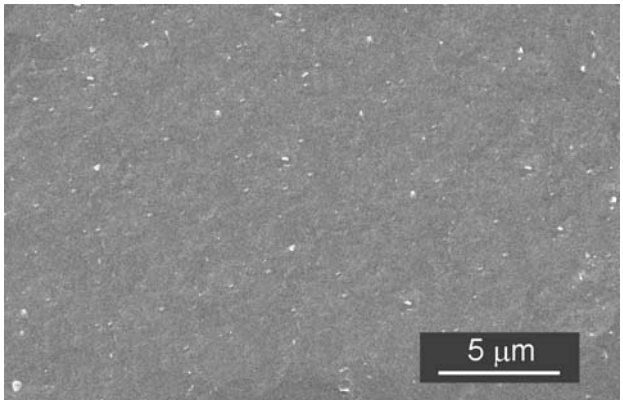


(a)

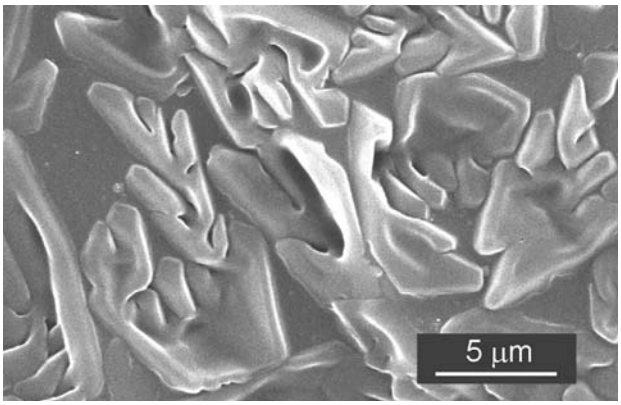


(b)

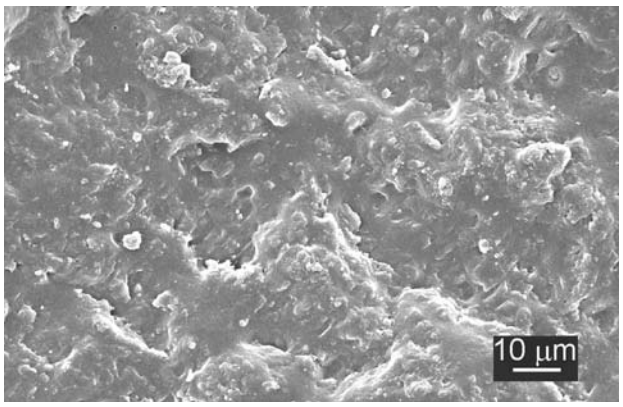


(c)

**Figure 6.** SEM photographs of: (a) neat XNBR, (b) XNBR/AO-2246 (40%), and (c) XNBR/AO-1010 (40%).

Besides, it should also be noted that a slight increase in the tan δ peak of XNBR is observed in compatible XNBR/AO-1010 systems in which the AO-1010 content is lower than 20%. According to relative studies, the initial increase of the tan δ peak of XNBR may be due to the positive effects of the

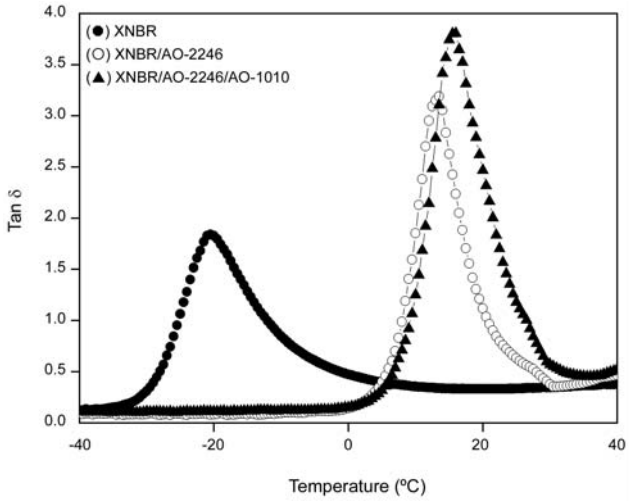


**Figure 7.** Temperature dependence of tan δ for XNBR, XNBR/AO-2246 (6:4) and XNBR/AO-2246 (6:4)/AO-1010 (10%).

addition of AO-1010 [29]. Another interesting point should be noted is that if a small amount of AO-1010 is incorporated into XNBR/AO-2246 hybrid, the damping peak height is further enhanced significantly and the peak position shifts to a higher temperature (as shown in Figure 7). This implies that AO-1010 and AO-2246 may have a synergistic effect on improving the damping property of XNBR. To confirm this suggestion, DMA measurements were carried out on various XNBR/AO-2246/AO-1010 ternary hybrids with fixed XNBR/AO-2246 weight ratio or fixed AO-1010 content.

Figure 8 shows the temperature dependence of tan δ for XNBR/AO-2246 (5:5) hybrids filled with various AO-1010 contents. As shown in this figure, the addition of 10% content of AO-1010 into XNBR/AO-2246 (5:5) hybrid leads to a significant increase of the damping peak maximum value (tan $\delta_{max}$) up to 4.0 and a notable enhancement of the damping peak temperature ($T_g$). With further increase in AO-1010 content, the tan $\delta_{max}$ begins to decrease rather than increase due to the partial compatibility of AO-1010 with XNBR. When the AO-1010 content exceeds 20%, the tan $\delta_{max}$ decreases sharply to a value of 2.8, which is lower than the unfilled XNBR/AO-2246 (5:5) hybrid. However, this value is still much higher than that of general damping material whose tan $\delta_{max}$ is often below 2.0. Moreover, the

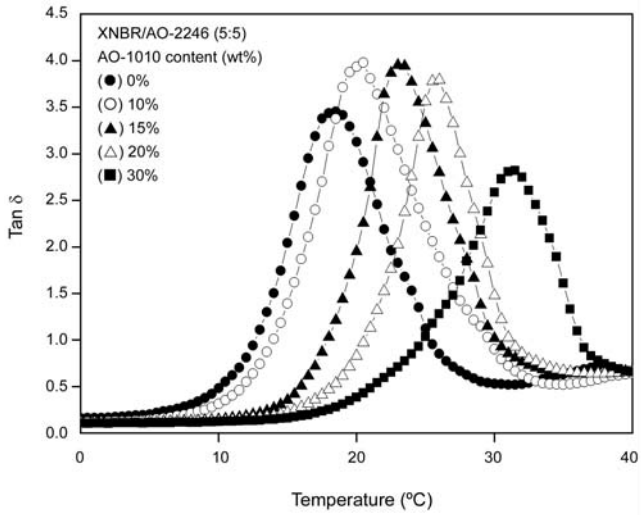


**Figure 8.** Temperature dependence of tan δ for XNBR/AO-2246 (5:5) hybrids filled with various AO-1010 contents.

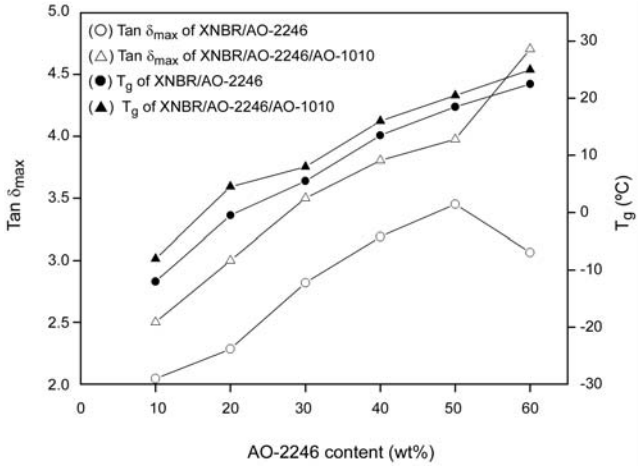


**Figure 9.** Comparison of the damping peak maximum value and its peak temperature for binary XNBR/AO-2246 and ternary XNBR/AO-2246/AO-1010 hybrids with a fixed AO-1010 content of 10%.

peak position is continuously shifted to a much higher temperature. These results suggest that both the tan $\delta_{max}$ and $T_g$ of XNBR/AO-2246 can be controlled by changing the addition content of AO-1010. The tan $\delta_{max}$ and $T_g$ of ternary XNBR/AO-2246/AO-1010 hybrids with a fixed AO-1010 content of 10% are compared with those of binary XNBR/AO-2246 in Figure 9. As shown in this figure, for any AO-2246 content, the addition of a small amount of AO-1010 into XNBR/AO-2246 leads to not only a remarkable increase in tan $\delta_{max}$, but also an enhancement of $T_g$. This further confirms that AO-1010 and AO-2246 indeed have a synergistic effect on enhancing the damping property of XNBR. Moreover, it can also be seen from Figure 9 that when the AO-1010 content is fixed at 10%, the tan $\delta_{max}$ and $T_g$ of ternary XNBR/AO-2246/AO-1010 hybrids increase significantly with increasing AO-2246 content. This suggests that at a fixed AO-1010 content, the damping properties of ternary XNBR/AO-2246/AO-1010 hybrids can be controlled by varying the XNBR/AO-2246 weight ratio. Thus, we can conclude that a series of high-performance damping materials with both high damping peak and controllable peak position suitable for different practical requirements may be designed and obtained by changing the composition of ternary XNBR/AO-2246/AO-1010 hybrids.

## Damping Stability of XNBR-based Organic Hybrids

As it is well known, the crystallization of additive molecules in a polymeric matrix during an ageing or heating process can frequently lead to the disappearance of their inherent functions as additives [29]. In addition, many researchers have revealed that small molecules such as 3,9-bis{1,1-dimethyl-2[β-(3-*t*-butyl-4-hydroxy-5-methylphenyl)propionyloxy] ethyl}-2,4,8,10-tetraoxaspiro[5,5]-undecane (AO-80) are easily crystallized in the presence of a solvent or polymer [30,31]. Thus, damping stability of the above organic hybrid damping materials during ageing or annealing process is of vital importance and needs to be examined further.

The damping peak maximum values of various XNBR/AO-2246 hybrids tested just one day after preparation (abbreviated as unaged samples) and those of the same samples tested after placing at room temperature for half a year against ageing (abbreviated as aged samples) are compared in Figure 10. It is evident from this figure that after ageing at room temperature for half a year, the tan $\delta_{max}$ of all XNBR/AO-2246 hybrids with different AO-2246 contents decreased.

As it is discussed above, the remarkable increase of tan $\delta_{max}$ of XNBR/AO-2246 hybrids is due to the formation of strong intermolecular hydrogen bonding

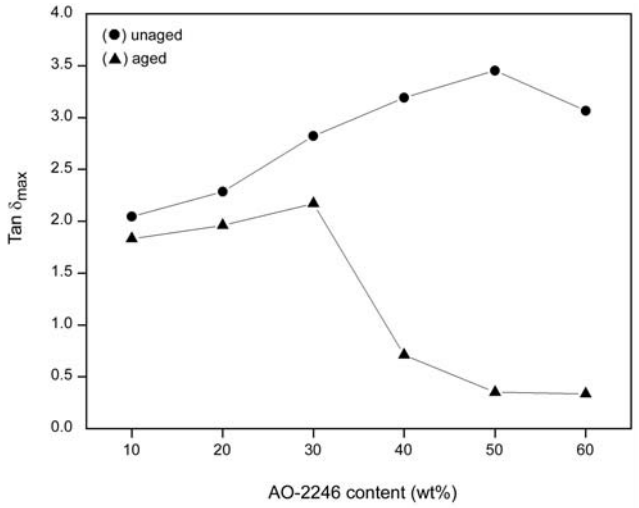


**Figure 10.** Comparison of damping peak maximum value of various unaged and aged XNBR/AO-2246 hybrids.

interactions between XNBR and AO-2246. Thus, it is reasonable to suppose that the decrease of tan $\delta_{max}$ may be attributed to the disappearance of such strong interactions. As shown in Figure 11, the new large broad centered band at 3375 $cm^{-1}$ corresponding to the OH–C=O intermolecular hydrogen bond between XNBR and AO-2246 decreases notably while the two characteristic sharp bands of pure AO-2246 centered at 3610 $cm^{-1}$ and 3389 $cm^{-1}$ increase remarkably, confirming the disappearance of strong intermolecular interactions and the release of a large amount of AO-2246 molecules. Therefore, tan $\delta_{max}$ of all XNBR/AO-2246 hybrids decreased remarkably.

Figure 12 shows the SEM photograph of the aged XNBR/AO-2246 (40%) sample. Compared with that of the same unaged sample as shown in Figure 6b, some AO-2246 crystal particles are formed during ageing due to the crystallization of AO-2246 molecules released by the disappearance of strong intermolecular hydrogen bonding interactions between XNBR and AO-2246. These AO-2246 crystal particles act as inorganic fillers and further decrease the tan $\delta_{max}$ sharply. Therefore, a much sharper decrease of the tan $\delta_{max}$ was observed in Figure 10 for the XNBR/AO-2246 samples with a larger AO-2246 content than 30%.

Further studies were performed on annealed XNBR/AO-2246 and XNBR/AO-2246/AO-1010 samples to investigate the additive effect of AO-1010

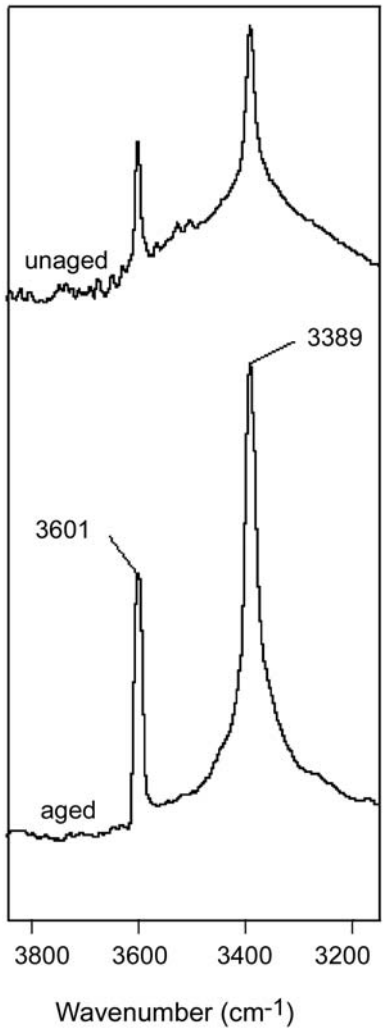


**Figure 11.** Infrared spectra in the OH stretching region for unaged and aged XNBR/AO-2246 (40%).

on the damping stability of XNBR/AO-2246 hybrid. The variations of tan $\delta_{max}$ for binary XNBR/AO-2246 (6:4) and ternary XNBR/AO-2246 (6:4)/AO-1010 (10%) hybrids annealed at 50ºC or 100°C for different annealing times are compared in Figure 13. As it is seen in this figure, tan $\delta_{max}$ of the annealed samples all decreases with increasing annealing time due to the phase separation resulting from the crystallization of AO-2246 molecules. It is noted that the tan $\delta_{max}$ of samples annealed at 100°C decreases much more gently than those annealed at 50°C. This is because at a higher temperature of 100°C, which is close to the melting point temperature of AO-2246 (127°C), most of the AO-2246 molecules are dissolved in the XNBR matrix uniformly in the form of molecules and

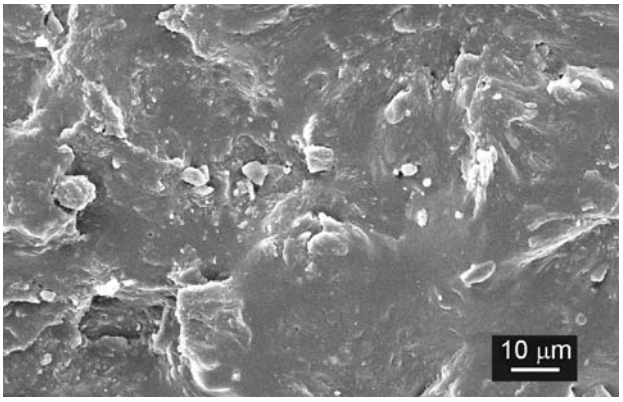


**Figure 12.** SEM photograph of aged XNBR/AO-2246 (40%) sample.

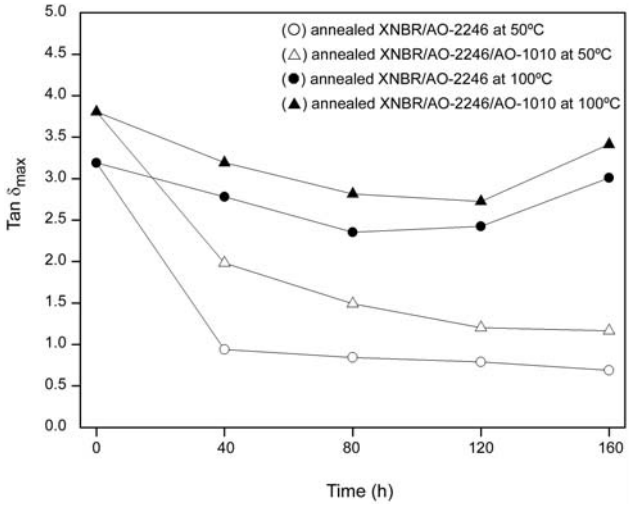


**Figure 13.** Time dependence of damping peak maximum value of binary XNBR/AO-2246 (6:4) and ternary XNBR/AO-2246 (6:4)/AO-1010 (10%) hybrids annealed at 50ºC or 100°C.

difficult to crystallize. In this case, the strong intermolecular hydrogen bonding interactions between XNBR and AO-2246 are kept to some extent. Thus, the decrease of the tan $\delta_{max}$ was slowed down. Another interesting point is also noted that after annealing at 100°C for more than 80 h, the damping

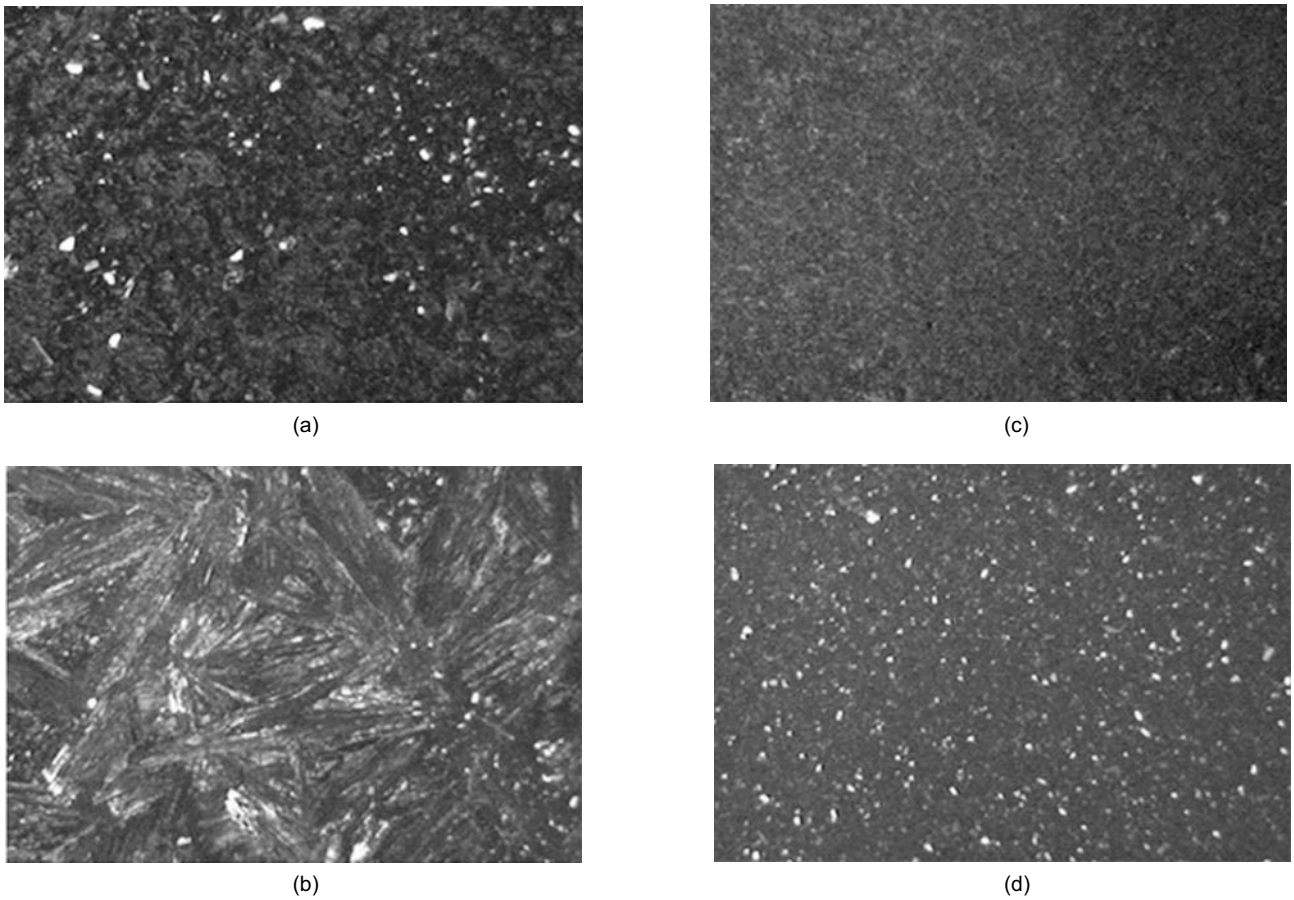


**Figure 14.** Optical micrographs of crystals at the surfaces for various samples annealed at 50ºC for 80 h: (a) XNBR/AO-2246 (6:4), (b) XNBR/AO-2246 (5:5), (c) XNBR/AO-2246 (6:4)/AO-1010 (10%), and (d) XNBR/AO-2246 (5:5)/AO-1010 (10%).

peak maximum reversely increases due to the heat-reversible effect of such organic hybrid, which will be reported in detail in a following paper.

Besides, it can also be observed from Figure 13 that compared with binary XNBR/AO-2246 hybrid, the decrease of the tan $\delta_{max}$ for ternary XNBR/AO-2246/AO-1010 is relatively slow and the tan $\delta_{max}$ at equilibrium is much higher. This suggests that the damping stability is improved by the addition of small amount of AO-1010. Since the decrease of the tan $\delta_{max}$ against annealing is mainly due to the crystallization of AO-2246 molecules, it is reasonable to assume that the improvement of the damping stability by AO-1010 may be attributed to the obstruction of the crystallization process. Several optical micrographs of crystals at the surfaces with a same magnification of 80 times for various samples annealed at 50°C for 80 h are compared in Figure 14. It may be noticed from this figure that after annealing at 50°C for 80 h, some AO-2246 crystals appear at the surfaces of XNBR/AO-2246 hybrid. In the case of XNBR/AO-2246 (6:4) sample, only a few polyhedron-shaped crystals can be seen at the surface, whereas a great number of large needle-shaped crystals are formed at the surface of XNBR/AO-2246 (5:5) sample due to the relatively larger local concentration of AO-2246 molecules at the surface. However, such growth form of crystals is changed by the addition of small amount of AO-1010. As it is seen in this figure, no crystal is formed at the surface of XNBR/AO-2246 (6:4)/AO-1010 (10%) while only some small polyhedron-shaped crystals rather than large needle-shaped crystals appear at the surface of XNBR/AO-2246 (5:5)/AO-1010 (10%). These results confirm that the crystallization behaviour of AO-2246 molecules in XNBR/AO-2246 hybrid is obstructed to a certain extent by the addition of small amount of AO-1010 molecules, which consequently improves the damping stability.

## CONCLUSION

In this paper, efforts have been made to prepare high-performance organic hybrid damping materials based on XNBR, which were chosen for the first time to be the polar matrix polymer in organic hybrid systems. Damping properties of some novel organic hybrids consisting of XNBR filled with large amounts of hindered phenols AO-2246 and AO-1010 were investigated. DMA results showed that binary system of XNBR/AO-2246 was compatible and only one damping peak associated with $T_g$ of XNBR appeared. With increasing AO-2246 content, the damping peak maximum value increased remarkably up to 3.5 and its peak position shifted towards higher temperature from -21°C to 23°C due to the hybridization of XNBR and AO-2246. FTIR analysis revealed that the hybridization effect was attributed to the formation of strong intermolecular hydrogen bonds between them. By contrast, binary XNBR/AO-1010 system was partially compatible due to weak intermolecular interaction between XNBR and AO-1010. When AO-1010 content was lower than 20%, single damping peak associated with $T_g$ of XNBR appeared and it was slightly increased.

However, when AO-1010 content exceeded 20%, two damping peaks were clearly observed, which can be assigned to the XNBR-rich domain and AO-1010-rich domain, respectively. With increasing AO-1010 content, the height of the first damping peak decreased sharply, but the height between the two damping peaks increased gradually, showing a broader efficient damping temperature region. FTIR results showed that both the number and strength of the intermolecular hydrogen bonding interactions formed in XNBR/AO-1010 system were much smaller than those of the intermolecular hydrogen bonding interactions formed in XNBR/AO-2246 system. SEM observation confirmed that such big differences in intermolecular interaction led to different dispersion state of AO-2246 and AO-1010 in XNBR matrix and finally resulted in different additive effects on damping properties of XNBR. Besides, DMA results of various ternary XNBR/AO-2246/AO-1010 systems showed that the addition of a small amount of AO-1010 into XNBR/AO-2246 further enhanced the damping peak height and peak temperature remarkably, demonstrating that AO-2246 and AO-1010 have a synergistic effect on improving the damping property of XNBR. Moreover, both the damping peak height and peak position of ternary XNBR/AO-2246/AO-1010 hybrid can be controlled by varying AO-1010 or AO-2246 contents.

On the other hand, studies on the damping stability of XNBR/AO-2246 hybrids against ageing showed that the damping peak height decreased sharply after ageing due to the formation of large amounts of AO-2246 crystals. FTIR analysis revealed that the crystallization of AO-2246 during ageing is attributed to the disappearance of strong intermolecular interactions between XNBR and AO-2246. Further studies on the damping stability of XNBR/AO-2246 and XNBR/AO-2246/AO-1010 organic hybrids during annealing process revealed that the addition of a small amount of AO-1010 into XNBR/AO-2246 obstructed the crystallization behaviour of AO-2246 to a certain extent and finally improved the damping stability.

Therefore, it can be concluded that a new type of XNBR-based organic hybrid high-performance damping materials with high damping peak and controllable peak position as well as better damping stability can be designed and obtained by changing the composition of ternary XNBR/AO-2246/AO-1010 hybrids.

## SYMBOLS AND ABBREVIATIONS

XNBR : carboxylated nitrile rubber
AO-2246 : 2,2'-methylenebis(6-*t*-butyl-4-methylphenol)
AO-1010 : pentaerythrityl-tetrakis-[β(3,5-di-t-butyl-4-hydroxyphenyl)-propionate]
tan δ : loss tangent
tan $\delta_{max}$ : damping peak maximum value
$T_g$ : damping peak temperature

## REFERENCES


1. Yin DH, Zhang Y, Peng ZL, Zhang YX, Effect of fillers and additives on the properties of SBR vulcanizates, *J Appl Polym Sci*, **88**, 775-782, 2003.
2. Ahmad A, Mohd DH, Abdullah I, Mechanical properties of filled NR/LLDPE blends, *Iran Polym J*, **13**, 173-178, 2004.
3. Frohlich J, Niedermeier W, Luginsland HD, The effect of filler-filler and filler-elastomer interaction on rubber reinforcement, *Composites Part A*, **36**, 449-460, 2005.
4. Soltani S, Sourki FA, Effect of carbon black type on viscous heating, heat build-up, and relaxation behaviour of SBR compounds, *Iran Polym J*, **14**, 745-751, 2005.
5. Semsarzadeh MA, Bakhshandeh GR, Ghasemzadeh-Barvarz M, Effect of carbon black on rate constant and activation energy of vulcanization in EPDM/BR and EPDM/NR blends, *Iran Polym J*, **14**, 573-578, 2005.
6. Ito M, Nagai K, Analysis of degradation mechanism of plasticized PVC under artificial aging conditions, *Polym Degrad Stab*, **92**, 260-270, 2007.
7. Shibata M, Teramoto N, Inoue Y, Mechanical properties, morphologies, and crystallization behavior of plasticized poly(*l*-lactide)/poly(butylene succinate-*co*-l-lactate) blends, *Polymer*, **48**, 2768-2777, 2007.
8. Ezzati P, Ghasemi I, Karrabi M, Azizi H, Correlation between the rheological behaviours and morphologies of PP/EPDM blends in various dynamic vulcanization systems, *Iran Polym J*, **17**, 265-272, 2008.
9. Ghanbarzadeh B, Oromiehie A, Musavi M, Razmi E, Milani J, Effect of polyolic plasticizers on rheological and thermal properties of zein resins, *Iran Polym J*, **15**, 779-787, 2006.
10. Wu CF, Yamagishi T, Nakamoto Y, Ishida S, Nitta K, Kubota S, Viscoelastic properties of an organic hybrid of chlorinated polyethylene and a small molecule, *J Polym Sci Part B: Polym Phys*, **38**, 1341-1347, 2000.
11. Wu C, Yamagishi T, Nakamoto Y, Ishida S, Nitta K, Kubota S, Organic hybrid of chlorinated polyethylene and hindered phenol. I. Dynamic mechanical properties, *J Polym Sci Part B: Polym Phys*, **38**, 2285-2295, 2000.
12. Wu CF, Yamagishi TA, Nakamoto Y, Ishida SI, Kubota S, Nitta KH, Organic hybrid of chlorinated polyethylene and hindered phenol. II. Influence of the chemical structure of small molecules on viscoelastic properties, *J Polym Sci Part B: Polym Phys*, **38**, 1496-1503, 2000.
13. Wu C, Yamagishi T, Nakamoto Y, Ishida S, Nitta K, Organic hybrid of chlorinated polyethylene and hindered phenol. III. Influence of the molec-

ular weight and chlorine content of the polymer on the viscoelastic properties, *J Polym Sci Part B: Polym Phys*, **38**, 2943-2953, 2000.
14. Wu CF, Organic hybrid of chlorinated polyethylene and hindered phenol. IV. Modification on dynamic mechanical properties by chlorinated paraffin, *J Polym Sci Part B: Polym Phys*, **39**, 23-31, 2001.
15. Wu CF, Otani Y, Namiki N, Emi H, Nitta KH, Kubota S, Dynamic properties of an organic hybrid of chlorinated polyethylene and hindered phenol compound, *J Appl Polym Sci*, **82**, 1788-1793, 2001.
16. Wu CF, Effects of a hindered phenol compound on the dynamic mechanical properties of chlorinated polyethylene, acrylic rubber, and their blend, *J Appl Polym Sci*, **80**, 2468-2473, 2001.
17. Wu CF, Akiyama S, Dynamic mechanical and adhesive properties of acrylate rubber/chlorinated polypropylene blends compatibilized with a hindered phenol compound, *Polym J*, **33**, 955-958, 2001.
18. Wu CF, Akiyama S, Enhancement of damping performance of polymers by functional small molecules, *Chin J Polym Sci*, **20**, 119-127, 2002.
19. Akasaka S, Shimura T, Sasaki S, Tominaga Y, Asai S, Sumita M, Viscoelasticity and morphology of an organic hybrid of chlorinated polyethylene and *N,N'*-dicyclohexyl-2-benzothiazolyl sulfenamide, *Compos Interf*, **12**, 637-653, 2005.
20. Zhang C, Sheng JF, Ma CA, Dynamic mechanical behavior of a novel polymeric composite damping material, *Chin Chem Lett*, **16**, 1527-1530, 2005.
21. Zhang C, Wang P, Ma CA, Sumita M, Damping properties of chlorinated polyethylene-based hybrids: effect of organic additives, *J Appl Polym Sci*, **100**, 3307-3311, 2006.
22. Li C, Xu SA, Xiao FY, Wu CF, Dynamic mechanical properties of chlorinated butyl rubber blends, *Eur Polym J*, **42**, 2507-2514, 2006.
23. Li C, Cao DM, Guo WH, Wu CF, The investigation of miscibility in blends of ENR/AO-80 by DMA and FT-IR, *J Macromol Sci Part B: Phys*, **47**, 87-97, 2008.
24. Zhao XY, Xiang P, Tian M, Fong H, Jin R, Zhang LQ, Nitrile butadiene rubber/hindered phenol nanocomposites with improved strength and high damping performance, *Polymer*, **48**, 6056-6063, 2007.
25. Ibarra L, Rodriguez A, Mora I, Ionic nanocomposites based on XNBR-OMg filled with layered nanoclays, *Eur Polym J*, **43**, 753-761, 2007.
26. Bandyopadhyay S, De PP, Tripathy DK, De SK, Influence of surface oxidation of carbon black on its interaction with nitrile rubbers, *Polymer*, **37**, 353-357, 1996.
27. Manoj NR, Chandrasekhar L, Patri M, Chakraborty BC, Deb PC, Vibration damping materials based on interpenetrating polymer networks of carboxylated nitrile rubber and poly(methyl methacrylate), *Polym Adv Technol*, **13**, 644-648, 2002.
28. Manoj NR, Raut RD, Sivaraman P, Ratna D, Chakraborty BC, Sequential interpenetrating polymer network of poly(ethyl methacrylate) and carboxylated nitrile rubber: dynamic mechanical analysis and morphology, *J Appl Polym Sci*, **96**, 1487-1491, 2005.
29. Wu CF, Yamagishi TA, Nakamoto Y, Crystallization behaviour of hindered phenol on chlorinated polyethylene matrix, *Polym Int,* **50**, 1095-1102, 2001.
30. Wu CF, Kuriyama T, Inoue T, Crystalline structure and morphology of a hindered phenol in a chlorinated polyethylene matrix, *J Mater Sci*, **39**, 1249-1254, 2004.
31. Wu CF, Akiyama S, Crystallization of a vitrified hindered phenol within chlorinated polyethylene and its effects on dynamic mechanical properties, *J Polym Sci Part B: Polym Phys*, **42**, 209-215, 2004.